Supporting information for

High-pressure Phase Transitions in Ordered and Disordered Bi_2Te_2Se

*Morten B. Nielsen[1], Paraskevas Parisiades[2], Solveig R. Madsen[1], Martin Bremholm[1]**

[1] Center for Materials Crystallography (CMC), Department of Chemistry and iNANO, Aarhus University, Langelandsgade 140, 8000 Aarhus C, Denmark

[2] European Synchrotron Radiation Facility, Beamline ID27, 71 Avenue des Martyrs, CS 40220, 38043, Grenoble Cedex 9, France

* Corresponding author. Email: bremholm@chem.au.dk

Contents of Supporting Information

Part 1 – 2D integrated dataset plot

Figure S1

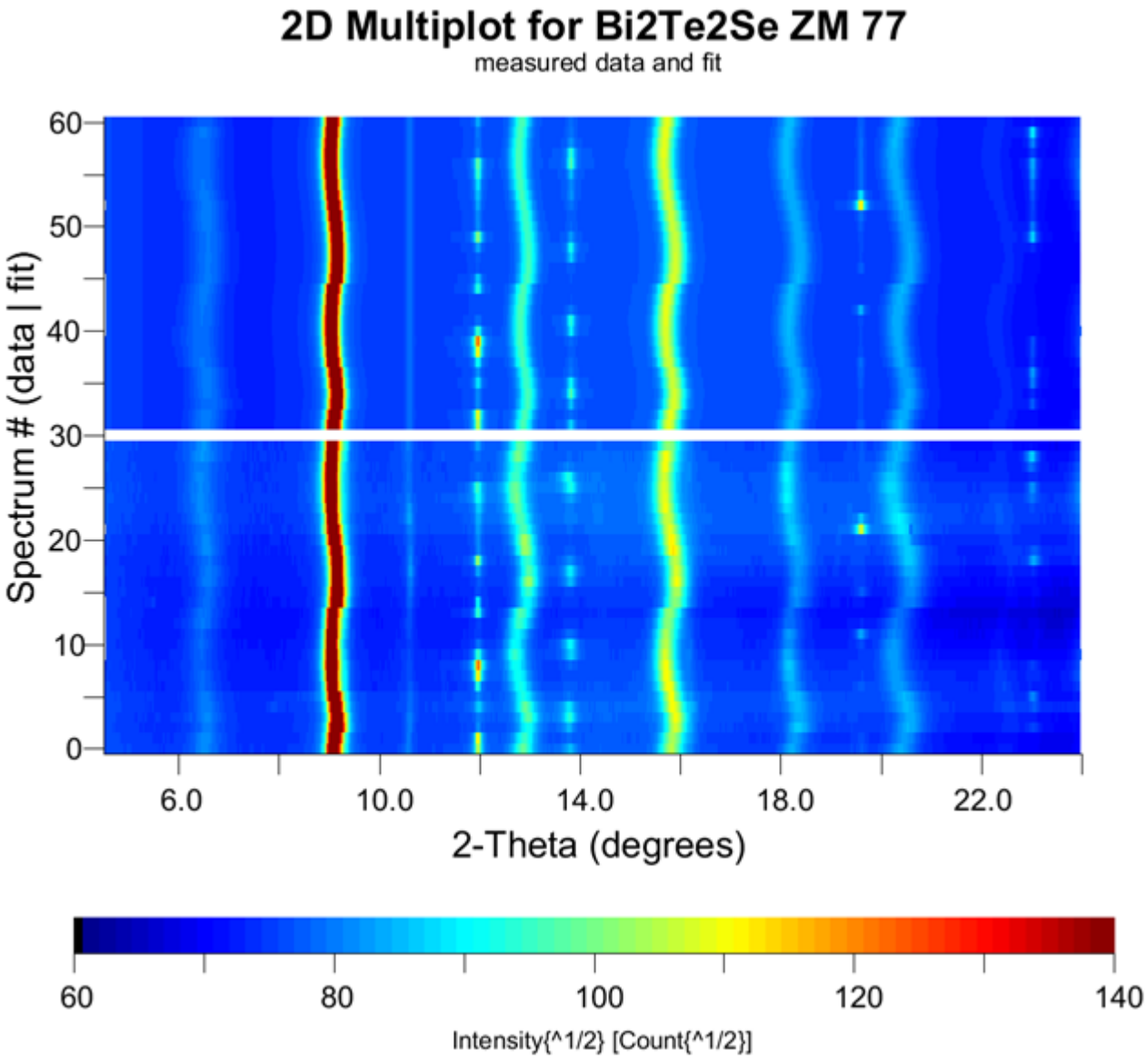

An example of an integrated high pressure dataset (bottom panel) and refinement (top panel) from the SB sample containing the δ phase at 57 GPa. Scattering angle makes up the first axis, azimuthal angle (going around the Debye-Scherrer ring) constitutes the second axis and the color scale shows the intensity. The wavy character of the sample diffraction lines is caused by the presence of strong anisotropic strain.

Part 2 – Raw data plots

Figure S2

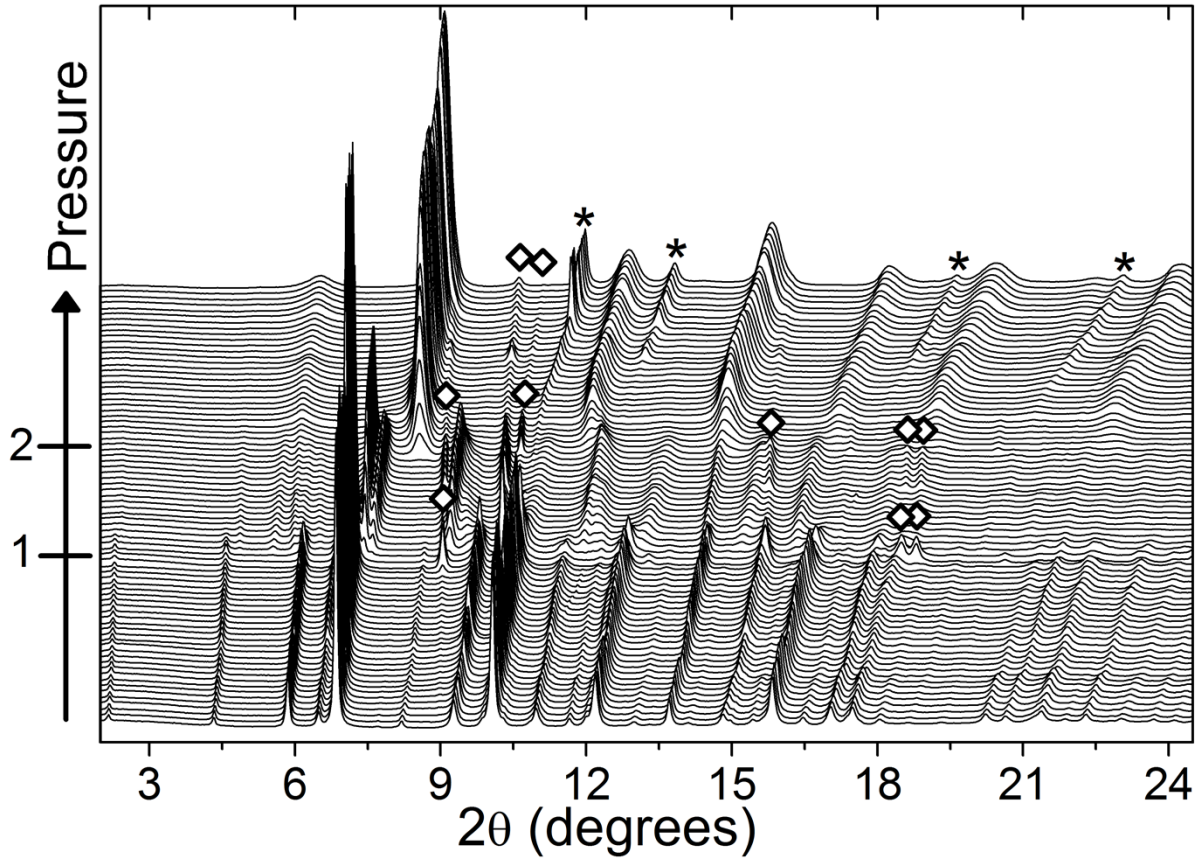

Full refined 2θ range plot of the raw data of the SB sample. Diamonds indicate diffraction peaks from the rhenium gasket, the asterisks indicate neon diffraction.

Figure S3

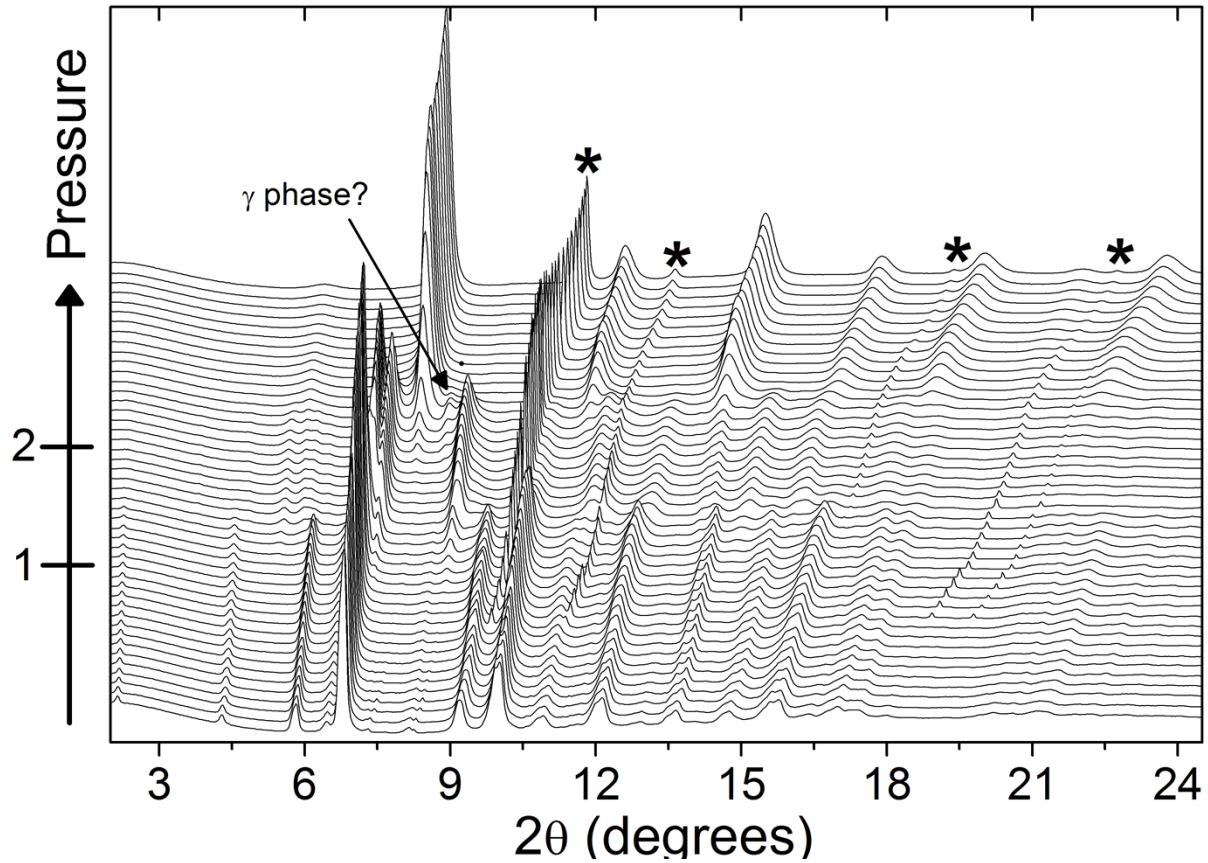

Full refined 2θ range plot of the raw data of the Q sample. The arrow indicates a cluster of diffraction peaks that fit with the γ-Bi_2Te_3 structure (though the data quality does not allow refinement), the asterisks indicate neon diffraction.

Part 2 – Refinement results

Table ST1

The full unit cell results versus pressure for both the SB and the Q sample.
SB sample data:

SB sample, α phase							
P	σ(*P*)	*a*	σ(*a*)	*c*	σ(*c*)	*V*/f.u.	σ(*V*)
0.84	0.01	4.264496	0.000072	29.6825	0.0019	155.83	0.14
0.86	0.01	4.259381	9.65E-05	29.61368	0.0025	155.09	0.18
1.12	0.01	4.252691	9.70E-05	29.52148	0.0025	154.13	0.18
1.59	0.01	4.240706	1.02E-04	29.3657	0.0027	152.45	0.19
1.76	0.02	4.235639	1.02E-04	29.30772	0.0027	151.79	0.19
2.01	0.02	4.228362	9.91E-05	29.24928	0.0025	150.96	0.18
2.40	0.02	4.219243	1.00E-04	29.16194	0.0020	149.86	0.14
2.71	0.02	4.211109	1.09E-04	29.06712	0.0027	148.80	0.19
3.45	0.03	4.193832	1.51E-04	28.92472	0.0029	146.86	0.21
3.72	0.03	4.187491	1.42E-04	28.86927	0.0029	146.13	0.20
3.81	0.03	4.180234	1.37E-04	28.8125	0.0026	145.34	0.18
4.36	0.03	4.173712	1.12E-04	28.75571	0.0012	144.60	0.09
4.65	0.04	4.16659	1.12E-04	28.72292	0.0012	143.95	0.08
4.94	0.04	4.16027	1.23E-04	28.67348	0.0015	143.26	0.10
5.16	0.04	4.154248	1.46E-04	28.64049	0.0024	142.68	0.17
5.55	0.04	4.14602	1.54E-04	28.59611	0.0018	141.90	0.12
5.81	0.04	4.140986	1.27E-04	28.54727	0.0013	141.31	0.09
6.09	0.05	4.134426	1.25E-04	28.51984	0.0013	140.73	0.09
6.47	0.05	4.129221	1.22E-04	28.4762	0.0012	140.16	0.08
6.79	0.05	4.122891	1.22E-04	28.43515	0.0012	139.53	0.08
7.14	0.05	4.115904	1.24E-04	28.39352	0.0013	138.85	0.09
7.49	0.06	4.10911	1.23E-04	28.36143	0.0027	138.24	0.18
7.98	0.06	4.099131	1.43E-04	28.31685	0.0026	137.35	0.17
8.59	0.07	4.086654	1.38E-04	28.25267	0.0025	136.21	0.17
8.81	0.07	4.081208	1.21E-04	28.2145	0.0013	135.66	0.09
9.15	0.07	4.074996	1.18E-04	28.18367	0.0027	135.10	0.18
9.50	0.07	4.069487	1.40E-04	28.15786	0.0016	134.61	0.11
10.06	0.08	4.061654	1.11E-04	28.11713	0.0023	133.90	0.15
10.60	0.08	4.050412	1.59E-04	28.05606	0.0029	132.87	0.19
10.92	0.08	4.045268	1.55E-04	28.04174	0.0029	132.47	0.19
11.36	0.09	4.037609	1.28E-04	28.04843	0.0026	132.00	0.17
11.87	0.09	4.029526	1.22E-04	27.99364	0.0022	131.21	0.14
12.12	0.09	4.020888	1.44E-04	27.99295	0.0023	130.65	0.15
13.03	0.10	4.011444	1.86E-04	27.93229	0.0030	129.75	0.20
13.52	0.10	4.010901	3.30E-04	27.90734	0.0051	129.60	0.33
13.96	0.11	3.991095	2.86E-05	27.86697	0.002362	128.140	0.152

SB sample, β phase

P	σ(*P*)	*a*	σ(*a*)	*b*	σ(*b*)	*c*	σ(*c*)	*β*	σ(*β*)	*V*/f.u.	σ(*V*)
11.87	0.09	14.34807	5.73E-04	3.996757	1.75E-04	17.0865	2.59E-04	148.7354	0.0017	127.13	0.35
12.12	0.09	14.33983	3.78E-04	3.987552	1.63E-04	17.05299	6.73E-04	148.7808	0.0021	126.35	0.45
13.03	0.10	14.31279	5.67E-04	3.977449	1.45E-04	17.00214	5.98E-04	148.7687	0.0019	125.46	0.39
13.52	0.10	14.30128	5.19E-04	3.959874	1.21E-04	16.95537	4.50E-04	148.6982	0.0014	124.72	0.28
13.96	0.11	14.29128	5.19E-04	3.949874	1.21E-04	16.91537	4.50E-04	148.6082	0.0014	124.34	0.28
14.36	0.11	14.2834	9.51E-04	3.92E+00	1.89E-04	16.86684	8.24E-04	148.5402	0.0025	123.07	0.51
14.74	0.11	14.2676	9.12E-04	3.909031	1.88E-04	16.8383	8.26E-04	148.5239	0.0025	122.59	0.50
15.23	0.12	14.23335	5.61E-04	3.905411	2.21E-04	16.80772	7.55E-04	148.4804	0.0025	122.11	0.50
15.63	0.12	14.21979	1.10E-03	3.897304	1.93E-04	16.77865	8.26E-04	148.484	0.0026	121.52	0.52
16.30	0.13	14.1741	0.001154	3.884991	2.14E-04	16.72542	8.58E-04	148.4381	0.0029	120.52	0.56
16.71	0.13	14.16411	9.38E-04	3.878494	2.25E-04	16.70154	5.39E-04	148.4282	0.0023	120.09	0.45
17.12	0.13	14.15638	9.73E-04	3.876359	2.22E-04	16.68548	8.41E-04	148.4117	0.0028	119.90	0.55
17.59	0.14	14.13189	8.33E-04	3.870805	2.18E-04	16.65068	6.76E-04	148.4364	0.0007	119.19	0.14
18.01	0.14	14.10639	0.001047	3.866533	2.25E-04	16.62504	8.56E-04	148.4244	0.0032	118.70	0.61
18.51	0.15	14.07748	8.20E-04	3.86149	2.32E-04	16.59255	4.32E-04	148.4013	0.0020	118.15	0.39
18.98	0.15	14.07169	9.32E-04	3.85369	2.07E-04	16.56933	7.95E-04	148.4112	0.0029	117.67	0.56
19.59	0.15	14.04522	0.001078	3.84206	2.35E-04	16.5237	9.20E-04	148.3111	0.0032	117.10	0.60
19.87	0.16	14.03987	0.001212	3.834779	2.66E-04	16.50466	0.001052	148.2933	0.0036	116.76	0.69
20.17	0.16	13.97029	0.002608	3.835278	5.85E-04	16.4635	0.001615	148.186	0.0082	116.25	1.53

SB sample, δ phase					
P	σ(*P*)	*a*	σ(*a*)	*V*/f.u.	σ(*V*)
19.59	0.15	3.544026	3.0E-04	111.283	0.028
19.87	0.16	3.54063	1.6E-04	110.964	0.015
20.17	0.16	3.539156	1.2E-04	110.825	0.011
20.50	0.16	3.538305	8.8E-05	110.745	0.008
20.82	0.16	3.535982	9.7E-05	110.527	0.009
21.21	0.17	3.533153	8.1E-05	110.262	0.008
21.49	0.17	3.529938	8.0E-05	109.962	0.007
22.05	0.18	3.525716	7.6E-05	109.568	0.007
23.03	0.18	3.520446	7.4E-05	109.077	0.007
23.11	0.19	3.517555	7.4E-05	108.808	0.007
24.01	0.19	3.510854	7.3E-05	108.188	0.007
25.72	0.21	3.499738	6.9E-05	107.163	0.006
27.37	0.22	3.488923	6.8E-05	106.173	0.006
29.04	0.24	3.477517	6.7E-05	105.135	0.006
30.42	0.25	3.468925	6.8E-05	104.358	0.006
32.04	0.26	3.45946	6.7E-05	103.506	0.006
33.70	0.28	3.444421	8.7E-05	102.162	0.008
34.69	0.29	3.438333	7.6E-05	101.621	0.007
36.93	0.31	3.432811	6.1E-05	101.132	0.005
39.57	0.33	3.419278	6.0E-05	99.941	0.005
42.01	0.36	3.406964	6.0E-05	98.865	0.005
43.08	0.37	3.399663	5.9E-05	98.231	0.005
44.78	0.39	3.392836	5.9E-05	97.640	0.005
46.20	0.40	3.387691	6.1E-05	97.197	0.005
50.05	0.44	3.368017	6.1E-05	95.513	0.005
51.01	0.45	3.364352	5.6E-05	95.202	0.005
53.14	0.47	3.354331	5.7E-05	94.353	0.005
55.25	0.49	3.34606	5.7E-05	93.657	0.005
56.94	0.51	3.338832	5.7E-05	93.052	0.005
58.67	0.53	3.331325	5.7E-05	92.425	0.005

Q sample, α phase

P	σ(*P*)	*a*	σ(*a*)	*c*	σ(*c*)	*V*/f.u.	σ(*V*)
0.18	0.01	4.301446	0.00013	29.9341	0.0024	159.88	0.18
0.49	0.01	4.293623	0.00013	29.8386	0.0024	158.79	0.17
1.23	0.01	4.271325	0.00010	29.5955	0.0022	155.87	0.16
1.71	0.01	4.258096	0.00013	29.4792	0.0024	154.30	0.17
2.09	0.02	4.246335	0.00013	29.3504	0.0024	152.77	0.17
2.59	0.03	4.232736	0.00013	29.2350	0.0022	151.20	0.16
3.12	0.03	4.218611	0.00012	29.1326	0.0020	149.67	0.15
3.52	0.04	4.206476	0.00012	29.0570	0.0020	148.42	0.14
4.16	0.03	4.192254	0.00013	28.9608	0.0022	146.93	0.16
4.74	0.04	4.181509	0.00013	28.8787	0.0023	145.77	0.16
5.42	0.04	4.169074	0.00013	28.8123	0.0022	144.57	0.15
5.81	0.04	4.155204	0.00013	28.7547	0.0022	143.32	0.15
6.39	0.05	4.144105	0.00013	28.6894	0.0022	142.23	0.15
7.18	0.05	4.129971	0.00012	28.6132	0.0021	140.89	0.14
7.73	0.06	4.116684	0.00013	28.5639	0.0022	139.74	0.15
8.67	0.07	4.098616	0.00012	28.4489	0.0023	137.96	0.16
9.11	0.07	4.087905	0.00012	28.3819	0.0022	136.92	0.15
9.58	0.07	4.076116	0.00012	28.3161	0.0022	135.81	0.15
10.30	0.08	4.06038	0.00013	28.2141	0.0024	134.28	0.16

Q sample, β phase

P	σ(*P*)	*a*	σ(*a*)	*b*	σ(*b*)	*c*	σ(*c*)	*β*	σ(*β*)	*V*/f.u.	σ(*V*)
13.54	0.10	14.29013	0.001428	3.973767	2.56E-04	16.98313	0.001043	148.5285	0.004281	125.87	0.88
14.24	0.11	14.25663	7.37E-04	3.96001	2.72E-04	16.94268	0.001035	148.5476	0.004495	124.78	0.92
14.75	0.11	14.22938	1.76E-03	3.955917	3.51E-04	16.91633	1.05E-03	148.5157	0.004586	124.33	0.93
15.27	0.12	14.24115	0.001645	3.949984	2.94E-04	16.87264	9.67E-04	148.4623	0.00348	124.11	0.70
15.93	0.12	14.22181	0.001191	3.924158	1.89E-04	16.84008	6.72E-04	148.4706	0.002321	122.87	0.47
16.70	0.13	14.19005	0.001902	3.910674	3.51E-04	16.75439	9.90E-04	148.4867	0.004057	121.49	0.80
17.12	0.13	14.18414	0.002021	3.908313	3.53E-04	16.75268	0.001074	148.4695	0.0041	121.42	0.81
17.66	0.14	14.15765	0.001436	3.893742	2.80E-04	16.70858	7.40E-04	148.413	0.002295	120.61	0.45
18.42	0.14	14.10887	3.29E-04	3.876632	2.07E-04	16.64589	4.80E-04	148.435	0.002253	119.15	0.44
19.72	0.16	14.05658	0.001428	3.851646	3.22E-04	16.54624	8.06E-04	148.3785	0.003254	117.42	0.62

SB sample, δ phase

P	σ(*P*)	*a*	σ(*a*)	*V*/f.u.	σ(*V*)
20.75	0.16	3.572415	1.09E-04	113.979	0.010
21.96	0.17	3.55997	9.07E-05	112.792	0.009
23.43	0.19	3.548711	8.49E-05	111.725	0.008
25.04	0.20	3.537706	8.20E-05	110.689	0.008
26.90	0.22	3.526833	8.11E-05	109.672	0.008
28.98	0.23	3.50893	8.24E-05	108.010	0.008
31.74	0.26	3.491611	7.99E-05	106.419	0.007
34.57	0.29	3.474197	7.68E-05	104.834	0.007
37.83	0.32	3.455109	7.46E-05	103.116	0.007
41.04	0.35	3.437752	7.29E-05	101.570	0.006
43.88	0.37	3.423111	7.12E-05	100.277	0.006
46.60	0.40	3.410337	7.03E-05	99.159	0.006
48.90	0.42	3.399661	6.99E-05	98.231	0.006

Part 3 – Rietveld refinements of the Q sample at 47 GPa, using various models.

Figure S4

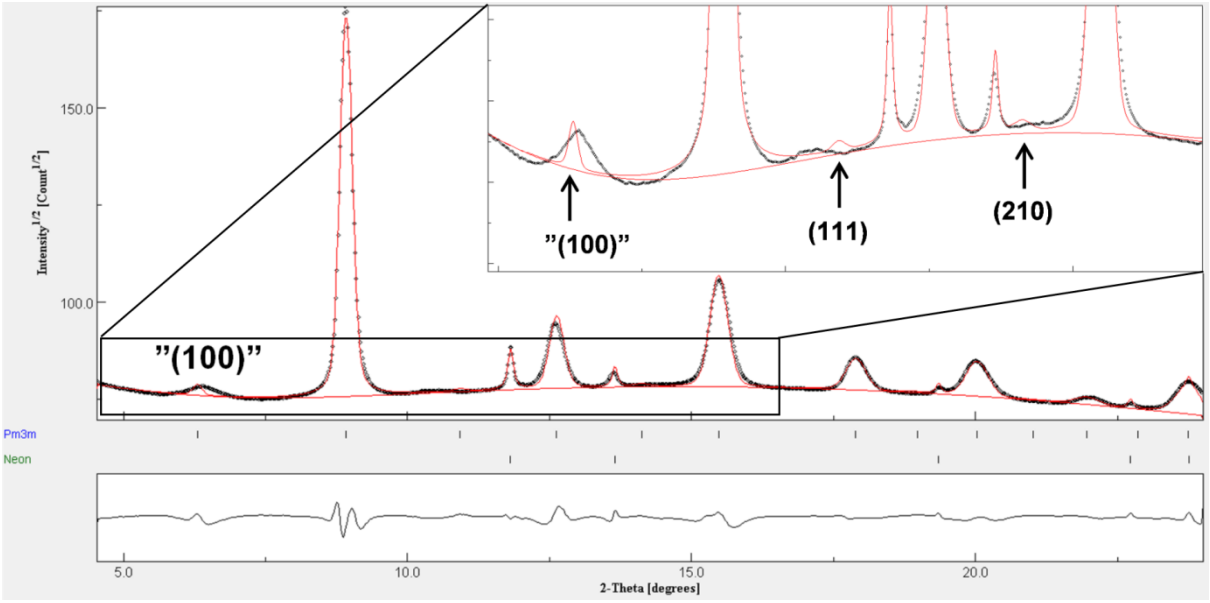

Model 1: A $Pm\bar{3}m$ space group, Bi/Te totally disordered, and with Se locked in the center of unit cell yields the fit in Fig. S3. The peak shape of the "(100)" reflection (~6.4 degrees) is to broad, leading to the total intensity of this peak being too low. Inset: A zoom in on the lower angle region, showing the lower intensity peaks. The broad signal at about 10.5 degrees corresponds to the main peak of rhenium (the gasket) at this pressure. Increasing the intensity of the "(100)" reflection would lead to increases in the (111) and (210) peaks that already describe too much intensity.

Model 2: Antiphasing

One effect that would only broaden the superstructure reflections appearing in going from $Im\bar{3}m$ to $Pm\bar{3}m$ is antiphase boundaries. The *hkl* dependence of this potential source of broadening can be calculated[13] as:

$$\beta(2\theta) = \frac{3}{2\mathrm{a}\cdot\cos(\theta)}\frac{\lambda\gamma(|h|+|k|+|l|)}{\sqrt{h^2+k^2+l^2}} \qquad \text{for } h+k+l = odd$$

In the equation, λ is the x-ray wavelength and γ is the probability of crossing an antiphase boundary within a given unit cell of length a. The expression assumes that γ is relatively small. The width predicted by this model scales with γ, but the relative widths of different peaks (such as (100) to (111)) is a constant. The width of a hypothetical (111) peak is thus 1.74 times that of the (100) peak.

Figure S5

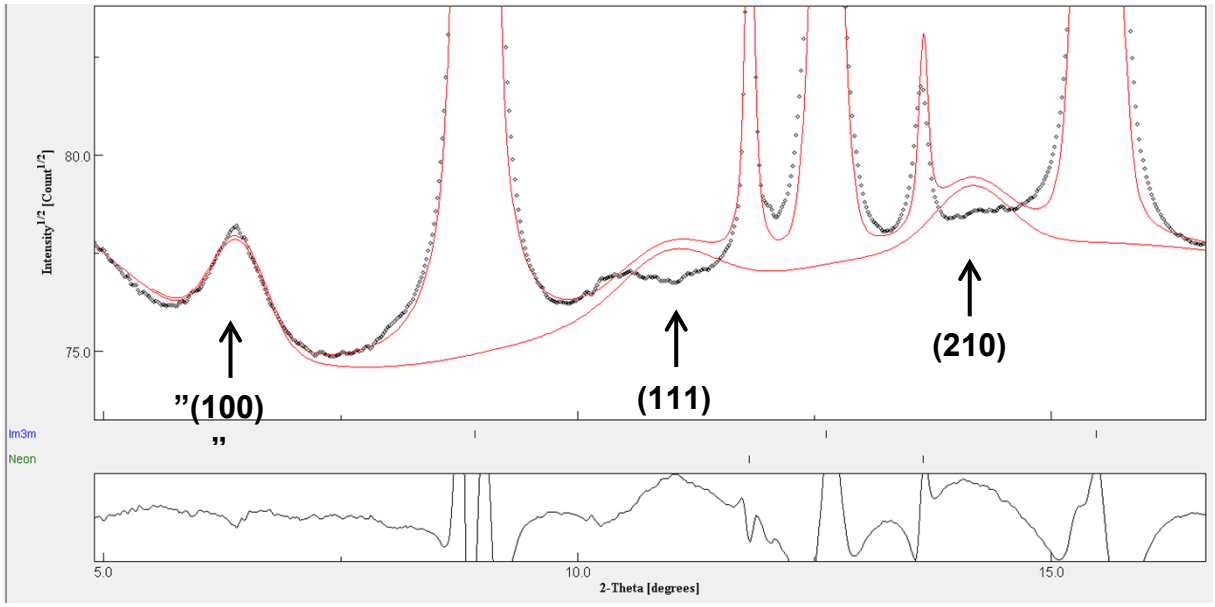

In Fig. S4 above we use the unit cell of the first model, but accounting for the broadening of the *h+k+l* = odd peaks that would arise from antiphase boundaries. The (100) peak has also been manually shifted to a much larger angle (i.e. no longer fits with the main peaks). Intensities of the 111 and 210 peaks are calculated from the observed intensity of the (100) peak based on the same model as before with Se only in the center of a Pm3m cell and total Bi/Te disorder over the remaining sites. The result is clearly too much intensity in the (111) and (210) peaks (again the broad signal at about 10.5 degrees fit with the main peaks of rhenium).

It should be noted that the width of the (100) peak is so large that the assumption of a low value of γ in the expression above likely breaks down.

Model 4 – A tetragonal unit cell

Figure S6

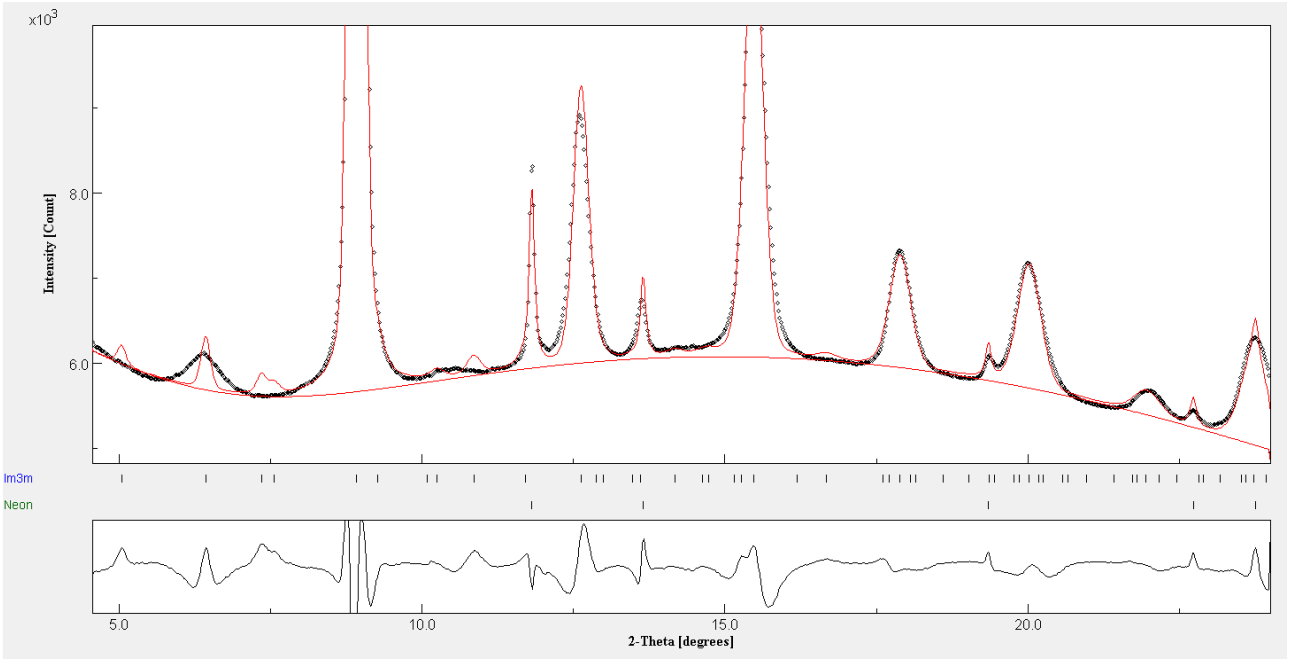

Bi_2Te_2Se as the *I4/mmm* cell claimed by Zhao *et al*. yields the fit in Fig. S6. Bi and Te were initially placed on the two 4*e* sites ((0,0,0.4003) for Bi and (0,0,0.2077) for Te) reported by Zhao *et al*. and then allowed to refine freely, including swapping sites. This leads to complete Bi/Te disorder over these two sites. Se was fixed to the 2*a* site at (0,0,0). The peaks at low angle (~5 and 7.5 degrees) that arise due to the lower tetragonal symmetry are definitely not present. However, this is the only case where the observed position of the "(100)" peak is in accordance with the model (the Miller index of the peak in this model is (101)). We have been unable to find atomic distributions that only remove the excess tetragonal peaks while keeping the "(100)" peak. The extra width of the "(100)" peak is also not accounted for in this model.